2D NMR Approaches to Characterizing the Molecular Structure and Dynamic Stability of the Active Site for Cyanide-Inhibited Horseradish Peroxidase

Zhigang Chen,[†] Jeffrey S. de Ropp,[‡] Griselda Hernández,[†] and Gerd N. La Mar*,[†]

Contribution from the Department of Chemistry and NMR Facility, University of California, Davis, California 95616

Received March 21, 1994[⊕]

Abstract: Cyanide-inhibited horseradish peroxidase, HRP-CN, has been investigated by 2D NMR in order to assign the signals for the active site residues and to determine their positions relative to each other and the heme. Analysis of the phase properties of COSY cross peaks reveals that cross correlation rather than coherence dominates for spatially close protons and that such cross peaks have limited use in identifying spin systems. It is shown, however, that TOCSY, particularly the CLEAN-TOCSY variant, is fully capable of mapping the spin systems for active site residues in low-spin ferric peroxidases. The prospects for detecting weak cross peaks from hyperfine shifted and paramagnetically relaxed, but unresolved, protons are significantly improved by combining WEFT or DEFT pulse-sequences with NOESY over a range of temperatures. Moreover, the presence of several very slowly exchanging labile protons for active site residues allows the standard sequence specific assignment of the proximal helical segment Gly 169-Phe 172, as well as part of Ser 167, and an unidentified residue in contact with the proximal His. Distal side assignments for the highly conserved Arg 38 and His 42 are revised and extended and the signals for Phe 41 located. The inter-residue and heme-residue dipolar contacts show that the position of the distal Arg and His are essentially the same as those in the crystal structures for lignin and cytochrome *c* peroxidases and that Phe 41 has an orientation similar to the homologous Phe in LiP. Identification of six labile protons with exchange lifetimes of several years at pH 7.0 in the holoprotein reveals that both the proximal and distal helices exhibit remarkable dynamic stability. The relevance of this NMR approach to other heme peroxidases is discussed.

Introduction

The heme peroxidases are a superfamily of enzymes which carry out one-electron oxidation at the expense of peroxides on a variety of structurally diverse substrates.[1,2] The two oxidizing equivalents imparted to the enzymes (compound I) by H_2O_2 are stored, one each, on the ferryl (Fe^{IV}=O) heme and as a cation radical either on the porphyrin or a nearby amino acid side chain; the intermediate one electron reduction product abolishes the radical and forms compound II. While the substrate binding site must differ significantly in the various peroxidases, the activation to compound I appears to be very similar.[2] Detailed structural studies over the past decade on the first crystallized heme peroxidase, yeast cytochrome *c* peroxidase,[3] *Cc*P,[4] have led to proposals that the catalytically important distal residues for classical peroxidases are Arg and His in a fragment Arg-X-Y-Arom-His on the distal side, the axial His, and a proximal Asp. The side chain interaction of the Asp imparts imidazolate character to the axial His which stabilizes the iron(IV) formed in the catalytic cycle.[3] Although overall sequence homology can be low, the catalytic amino acids appear to be highly conserved in the more extensive and diverse plant peroxidases.[5] More recently, the successful crystallization and structure determination of another fungal and a plant peroxidase, lignin peroxidase,[6] LiP, and the basic (E5) isozyme[7] of horseradish peroxidase, HRP, have shown that the remarkable sequence homology of the key catalytic residues is also manifested in structural homology, particularly in the active site. A schematic representation of the active site of HRP is shown in Figure 1.

In the absence of X-ray data, NMR spectroscopy has played a key role in elucidating the architecture of the active site in a variety of heme peroxidases.[8-18] Neither the relatively large size[1] (34-155 kDa) nor the ubiquitous paramagnetism make heme

[†] Department of Chemistry.

[‡] NMR Facility.

[⊕] Abstract published in *Advance ACS Abstracts*, September 1, 1994.

(1) For reviews, see: Dunford, H. B.; Stillman, J. S. *Coord. Chem. Rev.* **1976**, *19*, 187-251. Dunford, H. B. In *Peroxidases in Chemistry and Biology*; Everse, J., Everse, K. E., Grisham, M. B., Eds.; CRC Press: Boca Raton, FL, 1991; Vol. II, pp 1-24. Bosshard, H. R.; Anni, H.; Yonetani, T. In *Peroxidases in Chemistry and Biology*; Everse, J., Everse, K. E., Grisham, M. B., Eds.; CRC Press: Boca Raton, FL, 1991; pp 51-84. Welinder, K. G. In *Plant Peroxidases 1980-1990: Progress and Prospects in Biochemistry and Physiology*: Gaspar, T., Penel, C., Greppin, H., Eds.; University of Geneva Press: Geneva, Switzerland, 1992; pp 1-24.

(2) Ortiz de Montellano, P. R. *Annu. Rev. Pharmacol. Toxicol.* **1992**, *32*, 89-107.

(3) Poulos, T. L.; Kraut, J. *J. Biol. Chem.* **1980**, *255*, 8199-8205. Finzel, B. C.; Poulos, T. L.; Kraut, J. *J. Biol. Chem.* **1984**, *259*, 13027-13036.

(4) Abbreviations used: *Cc*P, cytochrome *c* peroxidase; HRP, horseradish peroxidase; LiP, lignin peroxidase; NOE, nuclear Overhauser effect; NOESY, 2D nuclear Overhauser spectroscopy; COSY, 2D correlation spectroscopy; MCOSY, magnitude correlation spectroscopy; P-COSY, 2D phase-sensitive correlation spectroscopy; TOCSY, 2D total correlation spectroscopy; ROESY, rotating frame nuclear Overhauser spectroscopy; DSS, 2,2-dimethyl-2-silapentane-5-sulfonate; WEFT, water-eliminated Fourier transformation; DEFT, driven equilibrium Fourier transformation; τ_{rd}, relaxation delay time in a WEFT or DEFT experiment.

(5) Welinder, K. G. *Eur. J. Biochem.* **1979**, *96*, 483-502. Welinder, K. G. *Eur. J. Biochem.* **1985**, *151*, 497-504. Welinder, K. G. *FEBS Lett.* **1976**, *72*, 19-23. Welinder, K. G.; Gajhede, M. In *Plant Peroxidases: Biochemistry & Physiology*; Welinder, K. G., Rasmussen, S. K., Penel, C., Greppin, H., Eds., 1993; pp 34-42.

(6) Edwards, S. L.; Raag, R.; Wariishi, H.; Gold, M. H.; Poulos, T. L. *Proc. Natl. Acad. Sci. U.S A.* **1993**, *90*, 750-754. Poulos, T. L.; Edwards, S. L.; Wariishi, H.; Gold, M. H. *J. Biol. Chem.* **1993**, *268*, 4429-4440.

(7) Morita, Y.; Funatsu, J.; Mikami, B. In *Plant Peroxidases: Biochemistry and Physiology*; Welinder, K. G., Rasmussen, S. K., Penel, C., Greppin, H., Eds.; University of Geneva Press: Geneva, Switzerland, 1993; pp 1-4.

(8) (a) de Ropp, J. S.; La Mar, G. N.; Smith, K. M.; Langry, K. C. *J. Am. Chem. Soc.* **1984**, *106*, 4438-4444. (b) Thanabal, V.; de Ropp, J. S.; La Mar, G. N. *J. Am. Chem. Soc.* **1987**, *109*, 265-272. (c) Thanabal, V.; de Ropp, J. S.; La Mar, G. N. *J. Am. Chem. Soc.* **1987**, *109*, 7516-7525. (d) Thanabal, V.; de Ropp, J. S.; La Mar, G. N. *J. Am. Chem. Soc.* **1988**, *110*, 3027-3035.

(9) Thanabal, V.; La Mar, G. N.; de Ropp, J. S. *Biochemistry* **1988**, *27*, 5400-5407.

(10) (a) de Ropp, J. S.; Yu, L. P.; La Mar, G. N. *J. Biomolec. NMR* **1991**, *1*, 175-192. (b) Sette, M.; de Ropp, J. S.; Hernández, G.; La Mar, G. N. *J. Am. Chem. Soc.* **1993**, *115*, 5237-5245.

(11) (a) La Mar, G. N.; de Ropp, J. S.; Smith, K. M.; Langry, K. C. *J. Biol. Chem.* **1980**, *255*, 6646-6652. (b) de Ropp, J. S.; La Mar, G. N. *J. Am. Chem. Soc.* **1991**, *113*, 4348-4350.

(12) Gonzalez-Vergara, E.; Meyer, M.; Goff, H. M. *Biochemistry* **1985**, *24*, 6561-6567.

0002-7863/94/1516-8772$04.50/0

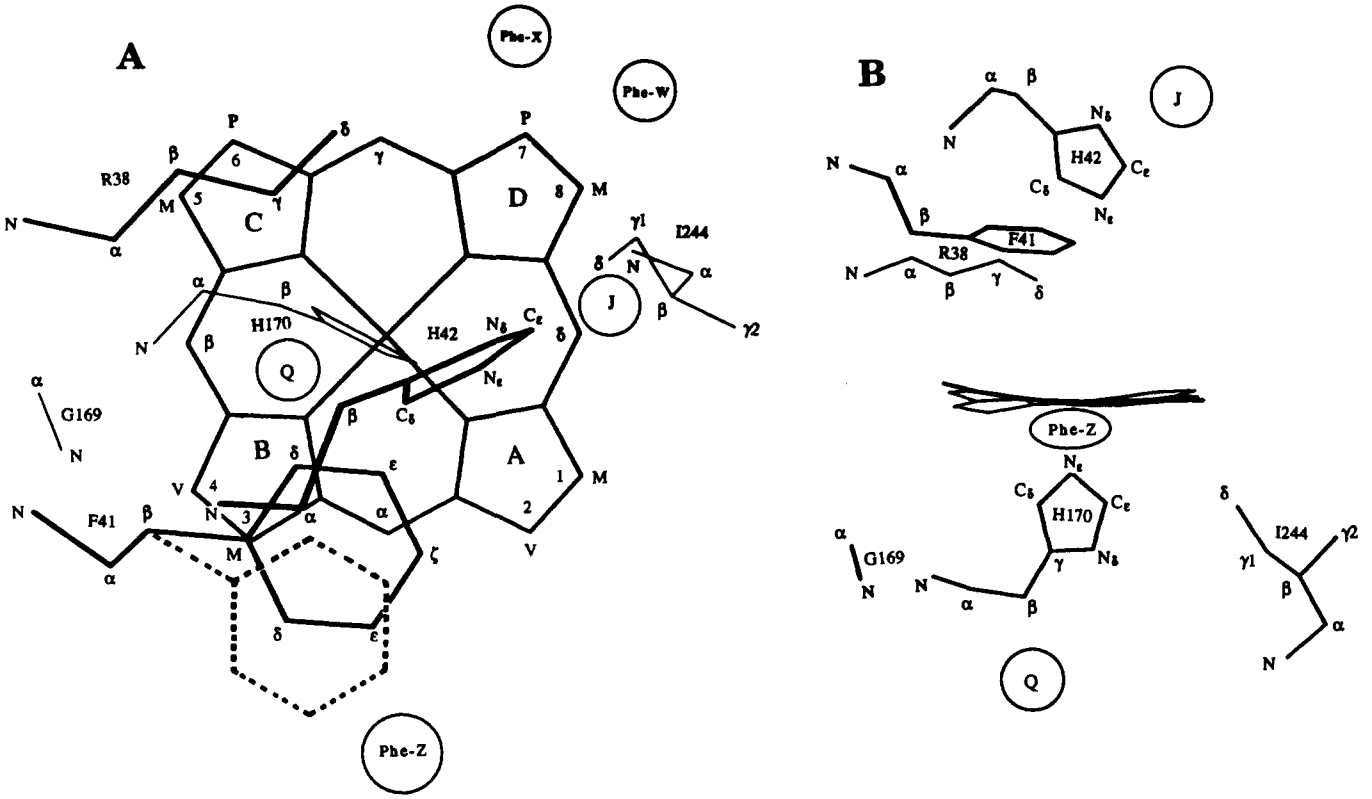

Figure 1. Heme pocket structure of HRP: (A) top view from the distal side, and (B) heme edge-on viewed from the α-meso position, for residues with protons expected <6 Å from the iron, as based on the crystal structure of C*c*P; the residues are identified for the HRP sequence. The distal Trp 51 of C*c*P[3] was substituted to Phe 41 of HRP with unaltered C_α–C_β rotational angle using the Biosym Insight-II program (Ala 174 and Leu 232 in C*c*P were similarly converted to Gly 169 and Ile 244, respectively). The position of the phenyl ring for Phe 41 relative to the heme corresponding to that in LiP[6] is indicated by dotted lines. The qualitative positions of several residues in contact with the heme edge, proximal His or distal His are shown in circles.

peroxidases ideal candidates for NMR investigation.[19] However, NMR provides not only detailed information on certain aspects of the molecular structure of the active site, but the hyperfine shifts resulting from the paramagnetism can yield unique information on the electronic structure of the various states of the enzyme.[8-18] NMR, moreover, has provided valuable information on both the location and dynamics of substrate binding.[16] While all forms of heme peroxidases yield useful ^{1}H NMR spectra, those for the low-spin cyanide complexes are by far the most informative because of narrow lines and large chemical shift dispersion for noncoordinated amino acids.[8,10,12-15,18]

The most extensively studied heme peroxidase is the neutral isozyme C of HRP, a 308 amino acid glycoprotein of 44 kDa (~21% glycosylated) which is considered prototypical of plant peroxidases.[1] A low-resolution single crystal structure of basic isozyme E5 is in progress.[7] Extensive ^{1}H NMR studies on isozyme C HRP-CN, first with isotope labeling,[8a] followed by steady-state NOE,[8b-d] and most recently by 2D NMR methods,[10,16b,e] have shown that HRP shares many similarities in both electronic and molecular structure with C*c*P. For C*c*P, the available crystal structure[3] provided an important guide for interpreting NMR data,[13] an advantage not yet shared by HRP. However, because of its much greater stability over broad ranges of pH and temperature, ^{1}H NMR has been much more definitively and successfully applied to both HRP[11] and HRP-CN.[8,10,16b,c] In fact, HRP and HRP-CN serve as benchmark systems for developing successful approaches to 2D NMR of large paramagnetic enzymes.[10,11b,19] Recent NMR studies of peroxidase point mutants[13a,d,17] make it even more important to refine and extend the necessary methodology.

The approach to solution NMR structure determination in large paramagnetic enzymes is necessarily the same as in small diamagnetic systems.[20] The unique side chain origin of signals of interest must be identified by a 2D scalar (spin) correlation (COSY, TOCSY) and the residues spatially defined relative to each other and to the heme via dipolar correlation (NOESY, ROESY). However, paramagnetic-induced relaxation can seriously undermine the efficiency of all 2D experiments both due to loss of coherence (short T_2s) and decreased NOEs (short T_1s).[19]

(13) (a) Satterlee, J. D.; Erman, J. E.; Mauro, J. M.; Kraut, J. *Biochemistry* **1990**, *29*, 8797–8804. (b) Satterlee, J. D.; Erman, J. E. *Biochemistry* **1991**, *30*, 4398–4405. (c) Satterlee, J. D.; Russell, D. J.; Erman, J. E. *Biochemistry* **1991**, *30*, 9072–9077. (d) Banci, L.; Bertini, I.; Turano, P.; Ferrer, J. C.; Mauk, A. G. *Inorg. Chem.* **1991**, *30*, 4510–4516.

(14) Goff, H. M.; Gonzalez-Vergara, E.; Bird, M. R. *Biochemistry* **1985**, *24*, 1007–1013. Shiro, Y.; Morishima, I. *Biochemistry* **1986**, *25*, 5844–5849. Thanabal, V.; La Mar, G. N. *Biochemistry* **1989**, *28*, 7038–7044. Dugad, L. B.; La Mar, G. N.; Lee, H. C.; Ikeda-Saito, M.; Booth, K. S.; Caughey, W. S. *J. Biol. Chem.* **1990**, *265*, 7173–7179.

(15) Lukat, G. S.; Rodgers, K. R.; Jabro, M. N.; Goff, H. M. *Biochemistry* **1989**, *28*, 3338–3345; de Ropp, J. S.; La Mar, G. N.; Wariishi, H.; Gold, M. H. *J. Biol. Chem.* **1991**, *266*, 5001–5008. Banci, L.; Bertini, I.; Turano, P.; Tien, M.; Kirk, T. K. *Proc. Natl. Acad. Sci. U.S.A.* **1991**, *88*, 6956–6960. Dugad, L. B.; Wang, X.; Wang, C.-C.; Lukat, G. S.; Goff, H. M. *Biochemistry* **1992**, *31*, 1651–1655. Banci, L.; Bertini, I.; Pease, E. A.; Tien, M.; Turano, P. *Biochemistry* **1992**, *31*, 10009–10017.

(16) (a) Sakurada, J.; Takahasi, S.; Hosoya, T. *J. Biol. Chem.* **1987**, *262*, 4007–4010. (b) Veitch, N. C.; Williams, R. J. P. *Eur. J. Biochem.* **1990**, *189*, 351–362. (c) Veitch, N. C.; Williams, R. J. P. In *Biochemical, Molecular and Physiological Aspects of Plant Peroxidases*; Lobarzewski, J., Greppin, H., Penel, C., Gaspar, T., Eds.; University of Geneva Press: Geneva, Switzerland, 1991; pp 99–109. (d) La Mar, G. N.; Hernández, G.; de Ropp, J. S. *Biochemistry* **1993**, *31*, 9158–9168. (e) Banci, L.; Bertini, I.; Bini, T.; Tien, M.; Turano, P. *Biochemistry* **1993**, *32*, 5825–5831.

(17) Veitch, N. C.; Williams, R. J. P.; Bray, R. C.; Burke, J. F.; Sanders, S. A.; Thorneley, R. N. F.; Smith., A. T. *Eur. J. Biochem.* **1992**, *207*, 521–531.

(18) Satterlee, J. D. *Annu. Rep. NMR Spectrosc.* **1986**, *17*, 79–178.

(19) La Mar, G. N.; de Ropp, J. S. In *Biological Magnetic Resonance*; Berliner, L. J., Reuben, J., Eds.; Plenum Press: New York, 1993; Vol. 12, pp 1–78.

(20) Wüthrich, K. *NMR of Proteins and Nucleic Acids*; Wiley & Sons: New York, 1986.

The NOESY experiment has been demonstrated to provide the necessary spatial contacts in HRP–CN, in several cases allowing quantitative distance determination.[10b] Early 2D NMR revealed surprising apparent effectiveness for detecting scalar connectivities in the form of the magnitude COSY, MCOSY experiment.[10a,13c,d] However, more recent considerations have shown that a mechanism exists for observing COSY peaks in large paramagnetic molecules that does not reflect scalar connectivity.[21,22] Hence, it is clear that a more careful evaluation of scalar correlation experiments on HRP–CN is in order. Previous studies have shown both 1D and 2D experiments to be effective for assigning the resolved hyperfine-shifted resonances.[8,10,13-15] However, a significant fraction of the hyperfine-shifted active site residues are not resolved outside the intense diamagnetic envelope, and their weaker cross peaks[19] are not readily identified in the presence of the more intense and larger number of cross peaks from the "diamagnetic" protons of the enzyme.

In this paper, we show that 2D experiments can be adapted to overcome most of the experimental problems encountered in large paramagnetic proteins such as HRP–CN, utilize the 2D experiments to provide definitive assignments of both previously identified as well as new residues in the heme pocket, and determine the stereochemistry of these residues in a semiquantative comparison with the crystal structure of CcP[3] and LiP.[6] In a separate study, we utilize these assignments and the determined strong structural similarity to CcP to develop an interpretive basis[23] of the hyperfine shifts that accounts qualitatively for the different NMR properties of structurally similar peroxidases in general and semiquantitatively for the influence of substrate binding on the NMR properties of HRP–CN in particular.

Experimental Section

Three mM solutions for NMR studies were prepared from HRP (>98% isozyme C) purchased from Boehringer-Mannheim as a lyophilized salt-free powder and dissolved directly into 99.9% ^2H_2O or 90%/10% H_2O/^2H_2O. HRP–CN was generated by addition of excess solid KCN to the protein solution. Solution pH was adjusted with small amounts of dilute ^2HCl or NaO^2H; pH values are not corrected for the isotope effect. Sample volumes of ca. 0.5 mL (for 5 mm tubes) and ca. 2.0 mL (for 10 mm tubes) were utilized. A sample of HRP–CN was also prepared from apoprotein soaked in ^2H_2O for several hours prior to reconstitution with heme, as described in detail previously.[8d] This results in the exchange with ^2H_2O of numerous labile peptide NH which otherwise exchange with ^2H_2O only over a period of years in the holoprotein.

NMR data were obtained over the temperature range 25–55 °C on a GE-NMR Ω-500 operating at 11.75 T. Steady-state NOE spectra were collected as described previously.[8b,c,14,16d] All chemical shifts were referenced to the chemical shift of water at the appropriate temperature, which in turn was calibrated against internal 2,2-dimethyl-2-silapentane-5-sulfonate, DSS. Magnitude COSY (MCOSY)[24] spectra were collected using 512 blocks in t_1 and ca. 300–800 scans per block. Phase-sensitive COSY (P-COSY),[25] TOCSY,[26,27] and NOESY,[28] spectra were collected with 512 blocks in t_1 using the hypercomplex method.[29] In general, 1024 or 2048 complex points in t_2 over a 20–31 kHz bandwidth were collected (in some of the scalar correlation experiments the downfield methyls were folded in). The solvent line was in all cases saturated during the predelay. All pulse sequences utilized here employed single (as opposed to composite) 90° hard pulses to maximize the bandwidth of excitation.[19] For experiments involving observation of hyperfine influenced resonances, a pulse sequence repetition rate of 5 s^{-1} was utilized as had been previously determined to be optimal.[10] For phase sensitive 2D data sets, the delay between pulse and acquisition of the first data point was adjusted to minimize the first-order phase correction in f_2.

In addition to the 2D sequences listed above, variants combining WEFT[30] or DEFT[31] into the initial portion of the pulse sequence were utilized; WEFT-NOESY and DEFT-NOESY[32] were found to be the most useful. In these pulse sequences the initial 90° pulse of NOESY is replaced by [180° – τ_{rd} – 90°] (for WEFT) or by [90° – τ_{rd} – 180° – τ_{rd}] (for DEFT), where τ_{rd} is the relaxation delay time. Selection of τ_{rd} to allow relaxation only for paramagnetically relaxed protons provides an effective spectral editing method for weakly relaxed protons. NOESY spectra were collected with mixing times ranging from 0.5 to 20 ms, the latter being the standard mixing time for data presented here.[10,19] TOCSY spectra were collected with mixing (spin lock) times of 6–22 ms. The MLEV-17 pulse train proved superior to WALTZ and DIPSI mixing schemes on our spectrometers for detection of coherence among hyperfine-influenced peaks and hence was used for all results presented here. To cover the broad range of hyperfine shifted peaks, spin lock fields of 25 kHz were used. The effect of trim pulse length was examined over the range 10 μs to 2 ms, and the optimal value was determined to be ca. 100 μs, with longer values reducing sensitivity of correlations to broad peaks and shorter values resulting in nonuniform phase across the spectrum. For CLEAN-TOCSY[27] the effect of varying the ROE suppressor delay was examined. Values of 1.0–4.0 were utilized with optimal performance found at the value of 2.6 as predicted;[27] this value was thus used for all data presented here.

Data sets were processed either on a SPARC II work station using GE-NMR Ω software 6.0 or on a Silicon Graphics 4D/35 using the Biosym software FELIX, versions 1.1 and 2.10. MCOSY data sets were processed with 0°-shifted sine-bell-squared apodization in both dimensions. TOCSY, NOESY, and P-COSY data sets were processed with 30–60°-shifted sine-bell-squared apodization in both dimensions. All data sets were zero-filled to 1024 × 1024 or 1024 × 2048 points. Phase-sensitive data were phase-corrected and base-line leveled in both dimensions. Further details of data processing are included in the relevant figure captions.

Results and Discussion

The Strategy. The ~50 protons on seven residues (and the heme) with at least one proton expected to be ≤6 Å (R_{Fe}) from the iron in the active site of HRP–CN (as inferred from sequence homology and the CcP and LiP crystal structures[3,5,6]) are characterized by two properties that distinguish them from the remaining ~3 × 10^3 protons: they possess shorter T_1s (∝ R_{Fe},[6] the iron–proton distance) and exhibit hyperfine shifts which are strongly temperature dependent.[33] Moreover, since at least the axial His 170 peptide NH exchanges sufficiently slowly with ^2H_2O that the signal is observed[8d] with full intensity after weeks in ^2H_2O, the possibility suggests itself that standard sequence-specific assignment[20] in ^2H_2O using backbone protons is feasible. In the next three sections we address experimental approaches to locating and assigning active site residues and in the subsequent three sections apply these methods to assign additional active site residues. In the last two sections, we draw conclusions as to the dynamics and structural properties of the active site of HRP–CN. Our target residues are those that exhibit strongly relaxed and/or hyperfine shifted protons (but not necessarily resolved from the diamagnetic envelope) and as many of the residues as possible which make contact with the heme and/or axial His 170. The heme and His 170 resonances have been definitively assigned previously.[8,10] Because the heme extends in-plane radially to 7 Å from the iron, some of the equatorial target residues may exhibit only marginal relaxation enhancement and/or hyperfine shifts. For this region, we will restrict the assignments to aromatic side

(21) Bertini, I.; Luchinat, C.; Tarchi, D. *Chem. Phys. Lett.* **1993**, *203*, 445–449.
(22) Qin, J.; Delaglio, F.; La Mar, G. N.; Bax, A. *J. Magn. Reson. Series B* **1993**, *102*, 332–336.
(23) La Mar, G. N.; Chen, Z.; Vyas, K.; de Ropp, J. S.; McPherson, A. D., submitted for publication.
(24) Bax, A. *Two-dimensional Nuclear Magnetic Resonance in Liquids*; Delft University Press: Dordrecht, Holland, 1982.
(25) Marion, D.; Wüthrich, K. *Biochem. Biophys. Res. Commun.* **1983**, *113*, 967–974.
(26) Braunschweiler, L.; Ernst, R. R. *J. Magn. Reson.* **1983**, *53*, 521–528.
(27) Griesinger, C.; Otting, G.; Wüthrich, K.; Ernst, R. R. *J. Am. Chem. Soc.* **1988**, *110*, 7870–7872.
(28) Macura, S.; Ernst, R. R. *Mol. Phys.* **1980**, *41*, 95–117.
(29) States, D. J.; Haberkorn, R. A.; Ruben, D. J. *J. Magn. Reson.* **1982**, *48*, 286–292.
(30) Patt, S. L.; Sykes, B. D. *J. Chem. Phys.* **1972**, *56*, 3182–3184. Lankhorst, P. P.; Wille, G.; van Boom, J. H.; Altona, C.; Haasnoot, C. A. G. *Nucl. Acids Res.* **1983**, *11*, 2839–2856.
(31) Becker, E. D.; Ferretti, J. A.; Farrar, T. C. *J. Am. Chem. Soc.* **1969**, *91*, 7784–7785.
(32) Kao, L.-F.; Hruby, V. J. *J. Magn. Reson.* **1986**, *70*, 394–407.
(33) Qin, J.; La Mar, G. N. *J. Biomolec. NMR* **1992**, *2*, 597–618.

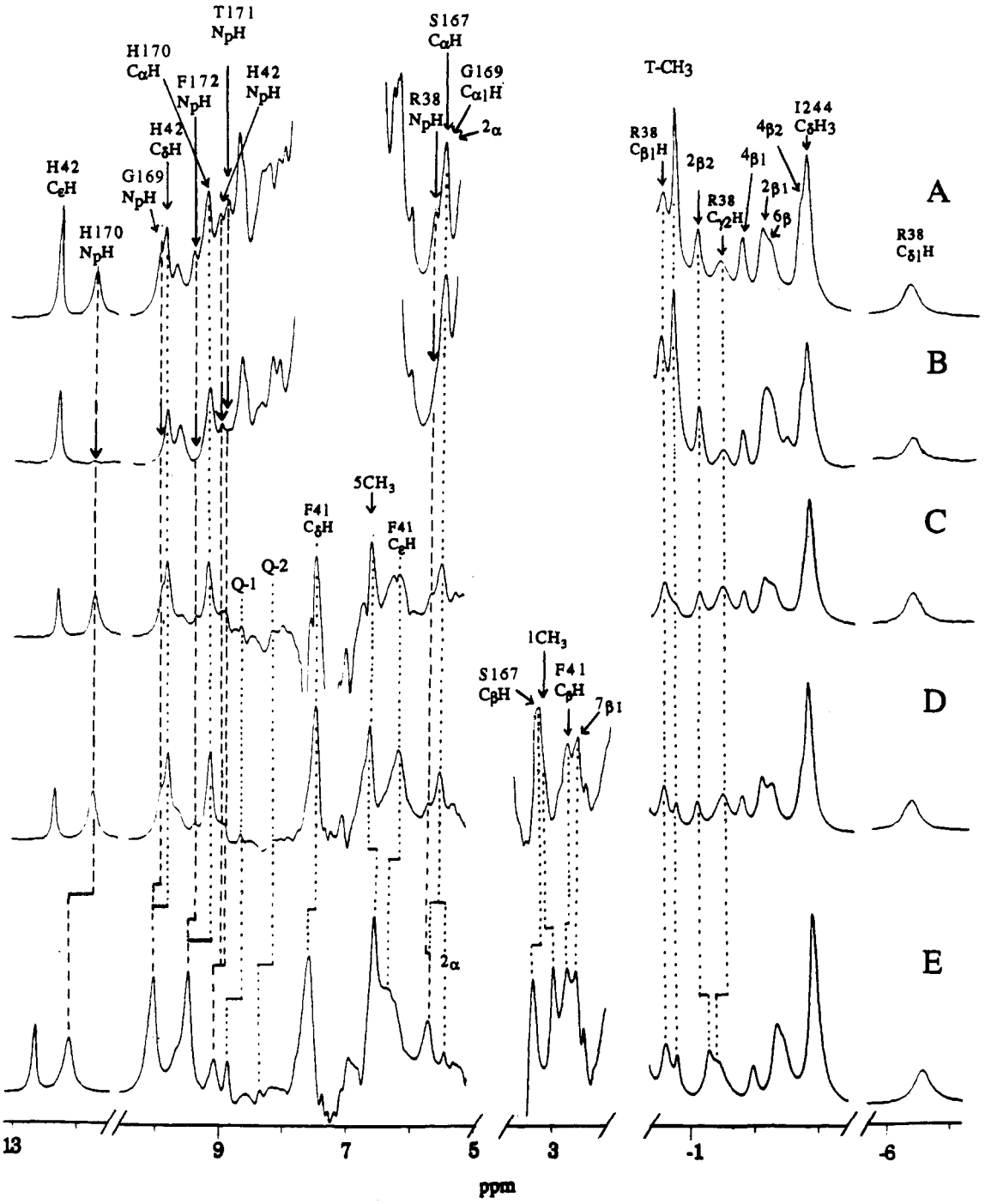

Figure 2. Portions of the 500 MHz ^{1}H NMR spectra of HRP–CN in ^2H_2O, pH 7.0: (A) normal (one-pulse) spectrum at 55 °C, (B) normal (one-pulse) spectrum of apo-HRP ^2H_2O exchanged HRP–CN, 55 °C, (C) WEFT spectrum of HRP–CN at 55 °C with τ_{rd} = 160 ms and repetition rate 5 s^{-1}, (D) DEFT spectrum of HRP–CN at 55 °C with τ_{rd} = 55 ms and repetition rate 5 s^{-1}, and (E) DEFT spectrum of HRP-CN at 45 °C; same conditions as in D. The vertical scale in the various spectra is such that the fully relaxed Arg $C_{\delta 1}H$ peak has comparable intensity. Slowly exchanging peptide NpHs are labeled by dashed lines; selected resonances that are enhanced in the WEFT/DEFT traces are labeled and connected by dotted lines. Assignments are described in the text.

chains, which are better resolved than the extremely crowded aliphatic region.

Emphasizing Active Site Residues. Pulse sequences such as WEFT[30] and DEFT[31] designed to suppress slowly relaxing solvent lines in the ^{1}H NMR of diamagnetic molecules can provide enormous improvements in the dynamic range for active site signals of paramagnetic proteins.[19,34] Active site residues exhibit[8c,d,10] a range of nonselective T_1s from <5 ms (the two axial His 170 ring CHs) to ~100 ms for protons at the heme periphery, R_{Fe} ~ 6–7 Å. The portion of the normal 500-MHz ^{1}H NMR spectrum near the diamagnetic window of HRP–CN in ^2H_2O, pH 7.0 at 55 °C is shown in Figure 2A; only the portion is shown where the envelope intensity is comparable to that of resolved peaks. Figures 2C and 2D provide WEFT and DEFT spectra designed to allow essentially complete relaxation only for peaks with $T_1 \leq 30$ ms. The upfield section in Figure 2A,C,D provides a reasonable calibration of the effect of the WEFT or DEFT pulse sequence, since the T_1s for all of these resonances have been reported;[8,10] least suppressed are the rapidly relaxed Arg 38 peaks ($T_1 \approx$ 15–60 ms), moderately suppressed are the four vinyl H_β peaks ($T_1 \approx$ 100 ms), and very strongly suppressed

(34) Emerson, S. D.; La Mar, G. N. *Biochemistry* **1990**, *29*, 1545–1556.

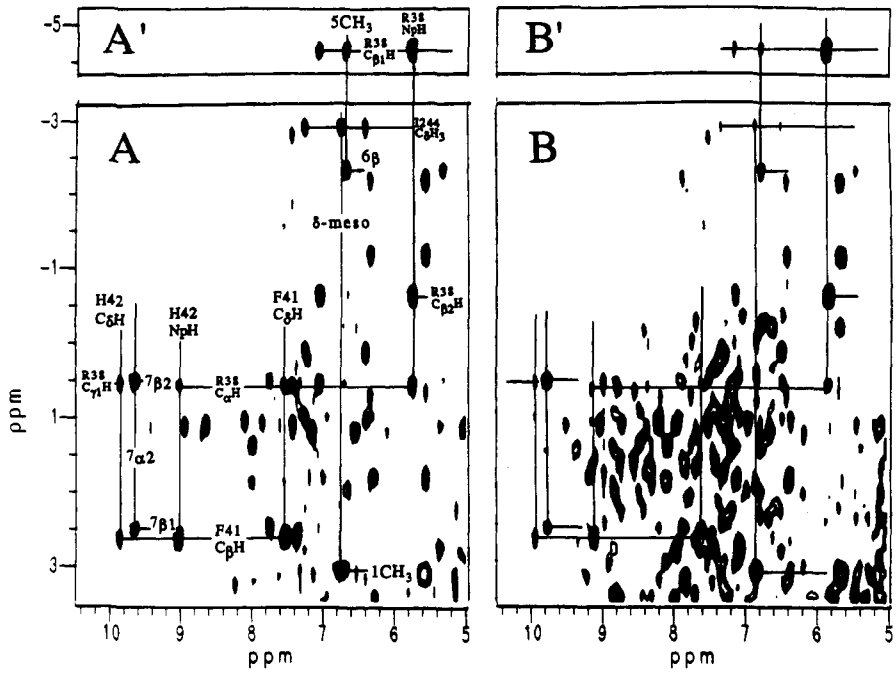

Figure 3. Comparison of portions of the 500 MHz NOESY spectra of HRP–CN in ^2H_2O, pH 7.0, 55 °C: (A, A′) WEFT-NOESY spectrum with τ_{rd} = 160 ms and repetition rate 5 s^{-1}, (B, B′) normal NOESY spectra, with repetition rate 5 s^{-1}. Both data sets utilized 20 ms mixing times. The data sets are scaled to exhibit comparable intensity for cross peaks involving strongly relaxed protons. Assignments (described in text) are given for several cross peaks on the WEFT-NOESY spectrum.

is the unassigned methyl peak at –0.74 ppm (T_1 > 150 ms). It is noted that the intensity of the bulk of the slowly relaxing aromatic window, 5–10 ppm, is either inverted (Figure 2C) or suppressed (Figure 2D), except for several prominent resonances which necessarily have T_1 < 100 ms. The DEFT trace in Figure 2D reveals the same resonances as in Figure 2C, except that it also allows the detection of four nonsuppressed resonances in the window 2–4 ppm which are obscured in the WEFT trace. Two of the previously assigned[8b,10a] unresolved heme methyl peaks, 1-CH_3 and 5-CH_3, are clearly detectable in the DEFT traces in Figure 2D,E. The DEFT trace at 45 °C in Figure 2E shows that each of the resonances revealed in Figure 2B-D exhibits temperature dependent shifts, as well as paramagnetic relaxation. Each of the emphasized resonances in Figure 2 are readily assigned (see below).

The preparation of the z-magnetization by a DEFT or WEFT pulse sequence can be combined with a 2D experiment.[32] Portions of crowded spectral windows of the normal NOESY map in Figure 3B,B′ are compared to WEFT-NOESY maps in Figure 3A,A′. The WEFT-NOESY map clearly enhances the intensities of cross peaks to hyperfine shifted signals (including those involving the relaxed peaks identified in Figure 2C,D), at the expense of those for the numerous cross peaks in the center of the figure that arise from slowly relaxing protons. Several enhanced cross peaks that are clear only in the WEFT-NOESY map, and which will be shown crucial in subsequent assignments, are labeled with lines. Similar results are obtained with DEFT-NOESY spectra (not shown). Hence, it is significantly easier to detect cross peaks for paramagnetically influenced protons in the 0–10 ppm window in a DEFT/WEFT-NOESY than normal NOESY map. Subsequent assignments are based on analyzing both normal and WEFT/DEFT-NOESY data collected over a range of temperatures to select for hyperfine shifted resonances which show temperature dependent chemical shifts. The obvious advantage of collecting variable temperature 2D data has been documented in detail previously.[19,33] A dramatic example of this advantage for HRP-CN is provided in the upfield MCOSY map (see supplementary material). The combination of WEFT methods and variable temperature studies will now be shown to provide assignments for the target residues of HRP–CN (see below). In all subsequent discussion, we address cross peaks between two resonances only if both exhibit detectable chemical shift changes over the temperature range 35–55 °C and the cross peaks are observed over a range of temperatures.

Scalar Correlation Experiments. Previous results from MCOSY spectra in the upfield region show[10a] cross peaks consistent with the seven nonlabile protons of an Arg spin system (Arg 38), but do the cross peaks reflect spin connectivity (coherence)? It has been shown that when a system exhibits ^1H NMR field dependent relaxation, there exists a cross correlation term with ^1H–^1H dipolar relaxation which is observed via cross peaks in a COSY experiment.[35] While such a field-dependent mechanism is rare for protons in diamagnetic systems, it is quite common in paramagnetic protein systems that are large and/or have a large S (Curie relaxation).[36] This was appropriately pointed out recently, and qualitative calculations of the scalar and cross correlation terms suggested[21] that the latter, rather than the former, dominated MCOSY cross peak intensities in high-spin resting state HRP. However, Qin *et al.* [22] have subsequently shown that coherence and cross-correlation contributions to COSY cross peaks are readily differentiated by their phase properties relative to the diagonal in the phase-sensitive form of the COSY experiment, P-COSY.[25] In phase-sensitive COSY, the in-phase diagonal components are $\pi/2$ out-of-phase with the anti-phase components of the cross peak due to coherence (J-coupling). In conventional P-COSY spectra, the diagonal is phased dispersive, making the cross peak antiphase absorptive (see ref 20, pp 68–72). For the present purposes, the diagonal is phased absorptive, making the J cross peak antiphase and dispersive.[22] In the limit of line width larger than J, the overlap of the two components leads to a single "up" coherence cross peak, as observed for the vinyl H_α–H_β cross peaks in Figure 4E. In contrast, the antiphase components of COSY cross peaks from cross correlation are in phase with the diagonal, and hence $\pi/2$ out-of-phase with J cross peaks.[22] This leads to cross peaks with the "up–down" pattern such as those observed for His 170 $C_{\beta 1}H$-$C_{\beta 2}H$ in Figure 4C,D.

(35) Wimperis, S.; Bodenhausen, G. *Mol. Phys.* **1989**, *66*, 897–919.
(36) Gueron, M. *J. Magn. Reson.* **1975**, *19*, 58–66. Vega, A. J.; Fiat, D. *Mol. Phys.* **1976**, *31*, 347–353.

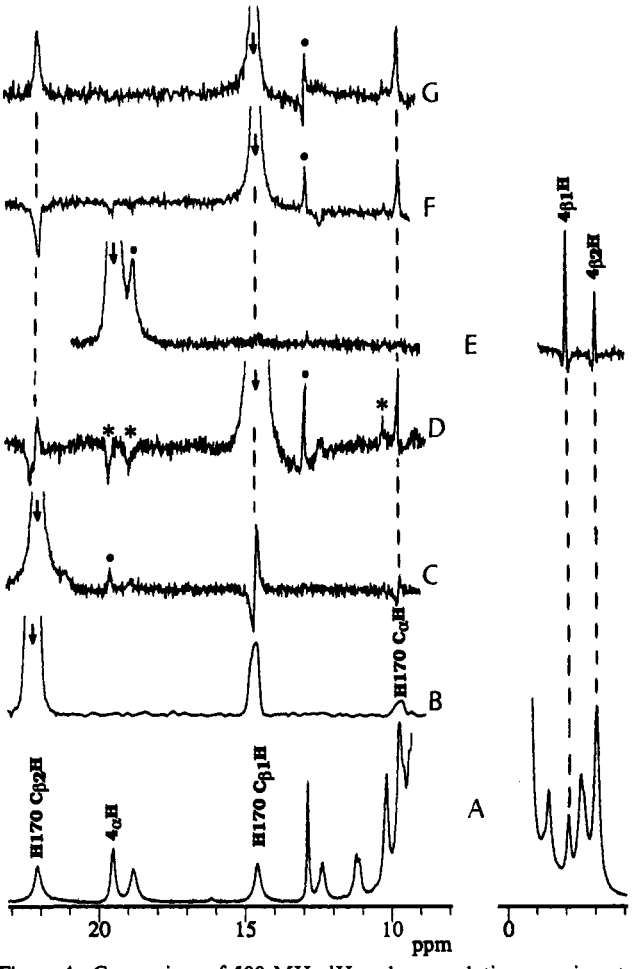

Figure 4. Comparison of 500 MHz ^{1}H scalar correlation experiments (MCOSY, P-COSY, TOCSY) for selected resonances of HRP–CN in ^2H_2O, pH 7.0, 40 °C. (A) Portions of the reference for resolved resonances. Traces B-G are f_2 slices through the labeled diagonal peak (marked by vertical arrow). (B) MCOSY slice at the His 170 $C_{\beta 2}H$ peak. (C) P-COSY slice for the His 170 $C_{\beta 2}H$ peak. (D) P-COSY slice for the His 170 $C_{\beta 1}H$ peak. (E) P-COSY slice for the 4-vinyl H_α ($\beta 1$ = βtrans, $\beta 2$ = βcis). (F) TOCSY (6 ms spin-lock) slice for the His 170 $C_{\beta 1}H$. (G) CLEAN-TOCSY (9 ms spin lock) slice for the His 170 $C_{\beta 1}H$. The slices B–G are plotted so that the diagonal peaks have the same intensity. Artifacts due to ridges are marked *, and off-resonance effects are marked ●.

Figure 4A shows the low-field and high-field portions of the 45 °C reference trace of HRP–CN in ^2H_2O, where the His 170 $C_\beta H_2$-$C_\alpha H$-N_pH fragment and the heme 4-vinyl group protons resonate.[8,10] Figure 4B shows the slice of the MCOSY map[10a] through the His 170 $C_{\beta 2}H$ resonance[37] illustrating the strong cross peak to its proposed geminal $C_{\beta 1}H$ partner and a weaker cross peak to its proposed vicinal $C_\alpha H$ partner. The same slice in a P-COSY map in Figure 4C with the diagonal phased pure absorptive, however, reveals that the cross peaks to both $C_{\beta 1}H$ and $C_\alpha H$ are due predominantly to cross correlation.[22] The slice of the P-COSY spectrum through the absorptive $C_{\beta 1}H$ diagonal (Figure 4D) exhibits a cross correlation peak to $C_{\beta 2}H$; however, the cross peak to $C_\alpha H$ in Figure 4D is a true COSY cross peak. The absorptive 4-H_α diagonal slice of the P-COSY spectrum in Figure 4E exhibits the phase of true COSY cross peaks[22] to 4$H_{\beta 1}$, 4$H_{\beta 2}$. The slices through Arg 38 $C_{\delta 1}H$ and $C_{\beta 1}H$ (not shown; see supplementary material) similarly show P-COSY cross peaks to their geminal partners which are due predominantly to cross correlation.[22]

Cross correlation qualitatively parallels cross relaxation, which is directly observed in NOESY spectra, and hence resonances exhibiting strong NOESY cross peaks in HRP–CN, such as geminal protons, have cross correlation dominating the P-COSY/MCOSY cross peak intensity. Even vicinal cross peaks are dominated by cross correlation if they exhibit a strong NOESY cross peak (*i.e.*, His 170 $C_{\beta 2}H$-$C_\alpha H$ in Figure 4C), while coherence dominates when the vicinal NOESY cross peak is weak (*i.e.*, H170 $C_{\beta 1}H$-$C_\alpha H$ in Figure 4D). Moreover, numerous MCOSY cross peaks are observed which can be readily shown to arise from spatially close, but not spin-coupled, protons[38] (see supplementary material). The above results lead to the conclusion that for low-spin, intermediate size (34–44 kDa) heme peroxidases,[8,10,12,13,15-17] the conventional COSY experiments have limited use for establishing geminal scalar connectivity.

The cross correlation effect is abolished by moving to the rotating frame TOCSY experiment.[26,27] However, here the problem is that the same experiment tends to simultaneously excite both the scalar (TOCSY) and dipolar (ROESY) responses, which, since they are 180° out-of-phase, can cancel each other.[39] For large proteins, where a stronger ROESY response (stronger cross relaxation) and a weaker TOCSY response (due to broader lines/shorter T_2s) are expected, detection of coherence can be difficult; but the prospects are improved by selecting very short mixing times.[19] The slice in the 6 ms mixing time TOCSY spectrum of HRP–CN through the His 170 $C_{\beta 1}H$ is shown in Figure 4F, which shows a weak TOCSY peak for $C_\alpha H$, but with a cross peak to $C_{\beta 2}H$ that is opposite in phase. This, and similar data (see supplementary material), reveal that in ordinary TOCSY[26] experiments in HRP–CN, the ROESY response dominates geminal partners, but vicinal couplings exhibit TOCSY response. However, with the CLEAN-TOCSY experiment[27] that is designed to suppress ROESY effects, the slice through $C_{\beta 1}H$ shown in Figure 4G now exhibits strong TOCSY response for both geminal and vicinal partners. Similar in-phase positive geminal and vicinal scalar cross peaks are observed in CLEAN-TOCSY spectra of HRP–CN for all expected hyperfine shifted peaks (see supplementary material for additional data), several of which will be considered in detail below. The use of significantly longer mixing times, *i.e.*, 22 ms (a routine value for diamagnetic systems),[26,27] resulted in the loss of all cross peaks to broad resonances (not shown). We therefore conclude that CLEAN-TOCSY with a short mixing time allows mapping of spin connectivity in ~34–44 kDa low-spin heme peroxidases.[8,10,12,13,17]

Sequence Specific Assignments. The spectral window where the amide and aromatic protons resonate for the NOESY map of HRP–CN in ^2H_2O at 45 °C is shown in Figure 5C. Inspection reveals a sequence of four dipolar-connected protons (labeled by arrows) that includes the His 170 peptide NH and whose chemical shifts suggest that they all arise from peptide NHs and form a series of sequential NH–NH NOEs typical of an α-helix.[20] Comparison of the reference trace of HRP–CN in ^2H_2O at 55 °C in Figure 2A with that of a similar sample prepared by reconstituting with heme a sample of apo-HRP which has been incubated[8d] in ^2H_2O, pH 8.0 at 20 °C for several hours (as shown in Figure 2B), confirms the intensity loss of these four labile protons. Hence the four proton NH_i–···, NH_{i+3} NOESY pattern[20] maps out the backbone for proximal residues for which the His 170 N_pH is NH_{i+1}. The low-field CLEAN-TOCSY spectrum (Figure 6) reveals two cross peaks for NH_i to protons which, in turn, exhibit both TOCSY (Figure 6) and intense NOESY (not shown; see supplementary material) cross peaks between them, uniquely identifying a Gly. This determines the direction of the proximal helix and unambiguously assigns residue i as Gly 169 from the known primary sequence.[5]

(37) The identification of stereospecifically assigned protons uses the labeling convention of the CcP crystal structure.[3]

(38) Several such resonances which exhibit MCOSY (and intense NOESY) cross peaks but will be shown to arise from non-spin-coupled proton pairs are His 170 $C_\beta H$-N_pH, His 42 $C_\delta H$-$C_\alpha H$ and $C_\delta H$-N_pH, Arg 38 $C_\beta H$-N_pH, and Phe 172 $C_\delta H$-N_pH, among others (see supplementary material).

(39) Kessler, H.; Griesinger, C.; Kerssebaum, R.; Wagner, K.; Ernst, R. R. *J. Am. Chem. Soc.* **1987**, *109*, 607–609.

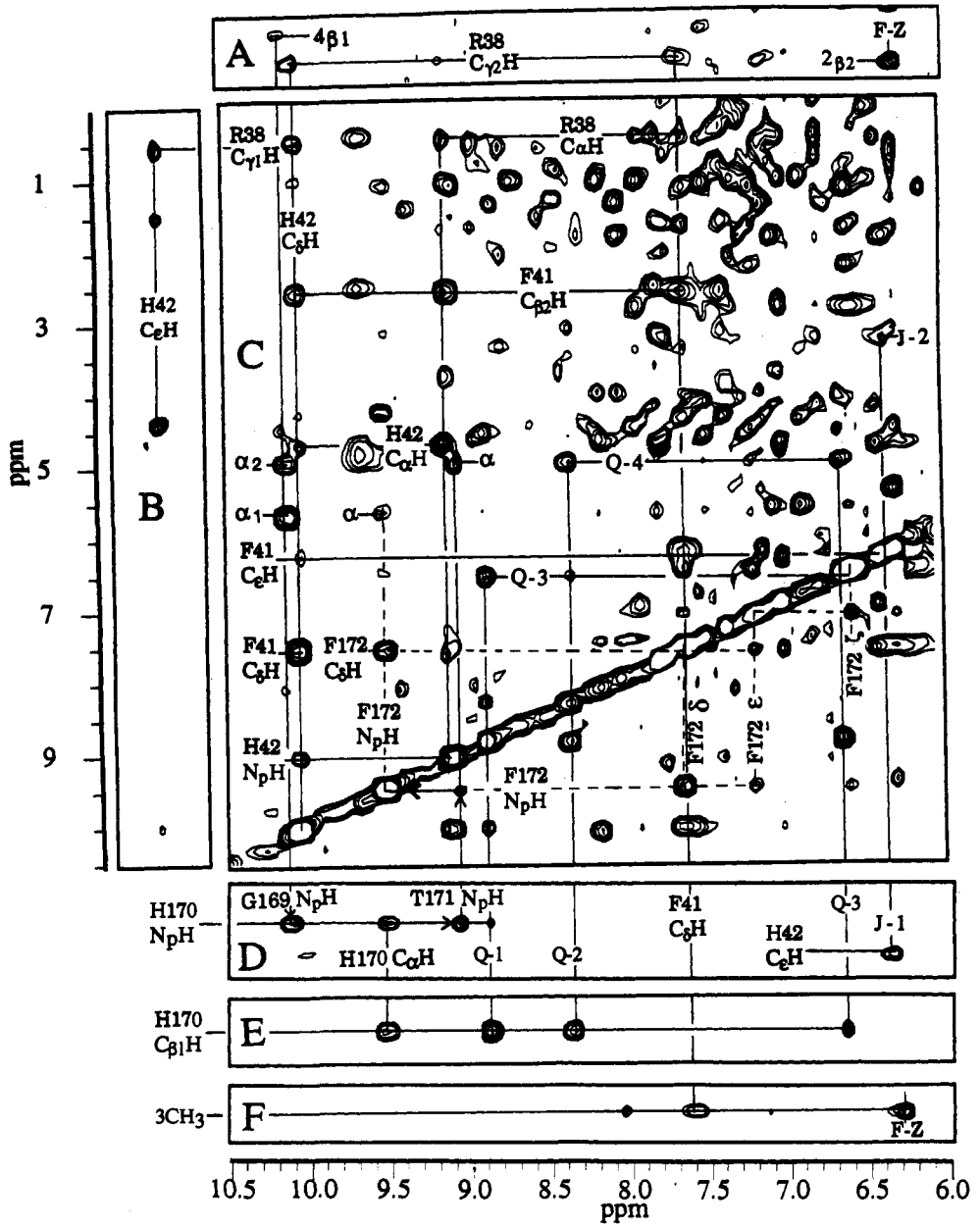

Figure 5. Portions of the 20 ms mixing time 500 MHz WEFT-NOESY spectrum of HRP–CN in ^2H_2O, pH 7.0, 45 °C; with τ_{rd} = 160 ms and a recycle rate of 5 s^{-1}. A system of lines with arrows (lower left of panel C, left part of panel D) shows the NH_i–NH_{i+1} connectivity pattern of residues 169–172. Cross peaks are connected by solid lines except for dashed lines for Phe 172. Assignments are given in text.

NH_{i+3} (predicted to be Phe 172 from the sequence[5]) exhibits a TOCSY cross peak to its $C_\alpha H$ (Figure 6), but spectral congestion precludes mapping out the $C_\beta Hs$. The NH_{i+3}, however, exhibits a very strong NOESY cross peak[38] to a peak at 7.61 ppm at 45 °C and a weak cross peak to 7.16 ppm (Figure 5C) which the TOCSY pattern (Figure 6), chemical shifts, and variable temperature intercepts (Table 1) reveal to arise from a rapidly reorienting phenyl side chain. The strong NOEs from the NH to $C_\delta Hs$ (and weak to $C_\epsilon Hs$) dictate that this is the expected phenyl side chain for Phe 172 and further confirms the identity of the helical sequential NH_i–N_{i+1} dipolar connectivities for the segment Gly 169-Phe 172. The chemical shifts for the identified protons on these residues are listed in Table 1. The cross peak from Gly 169 NH to Gly 168 NH was not detected. However, an additional temperature dependent and moderately relaxed spin system is located on the proximal side for which the two protons at 5.73 and 3.26 ppm exhibit TOCSY (Figure 6) and NOESY cross peaks between each other, with the 5.73 ppm peak displaying moderate intensity NOESY cross peaks to the His 170 $C_\beta Hs$ (see supplementary material). Both peaks exhibit significant intensity in the WEFT and DEFT traces (Figure 2C,D), indicating proximity (<7 Å) to the iron. The NOE to the His 170 $C_\beta Hs$ is that expected for the $C_\alpha H$ of Ser 167 via the classic α_i–β_{i+3} dipolar connectivity[20] on an α-helix. Hence, the residue is tentatively assigned as Ser 167 with the 3.26 ppm peak attributed to a $C_\beta H$; the third side chain proton was not located. The *Cc*P[3] and LiP[6] crystal structures place the analogous $C_\alpha H$ (Met 172 in *Cc*P; Leu 173 in LiP) only ~6 Å from the iron, consistent with the relaxation properties of the 5.73 ppm peak.

Other Proximal Residues. The detailed stereospecific assignment of His 170 protons on the basis of NOE and NOESY data has been reported;[10b] the present TOCSY data confirm the spin connectivity for the $NHC_\alpha HC_\beta H_2$ fragment (Figure 4F,G). Protons for Gly 169, Phe 172, and Ser 167 were assigned in the previous section. The upfield methyl peak at −2.87 ppm had been shown to result from a proximal side residue on the basis of a strong NOE from the axial His 170 $C_\epsilon H$[8c] and placed near the heme edge at the junction of pyrrole A and D by NOEs and NOESY cross peaks[10a] to 1-CH_3 and 8-CH_3. The detection of two TOCSY peaks to the methyl uniquely identifies a $C_\delta H_3$ of

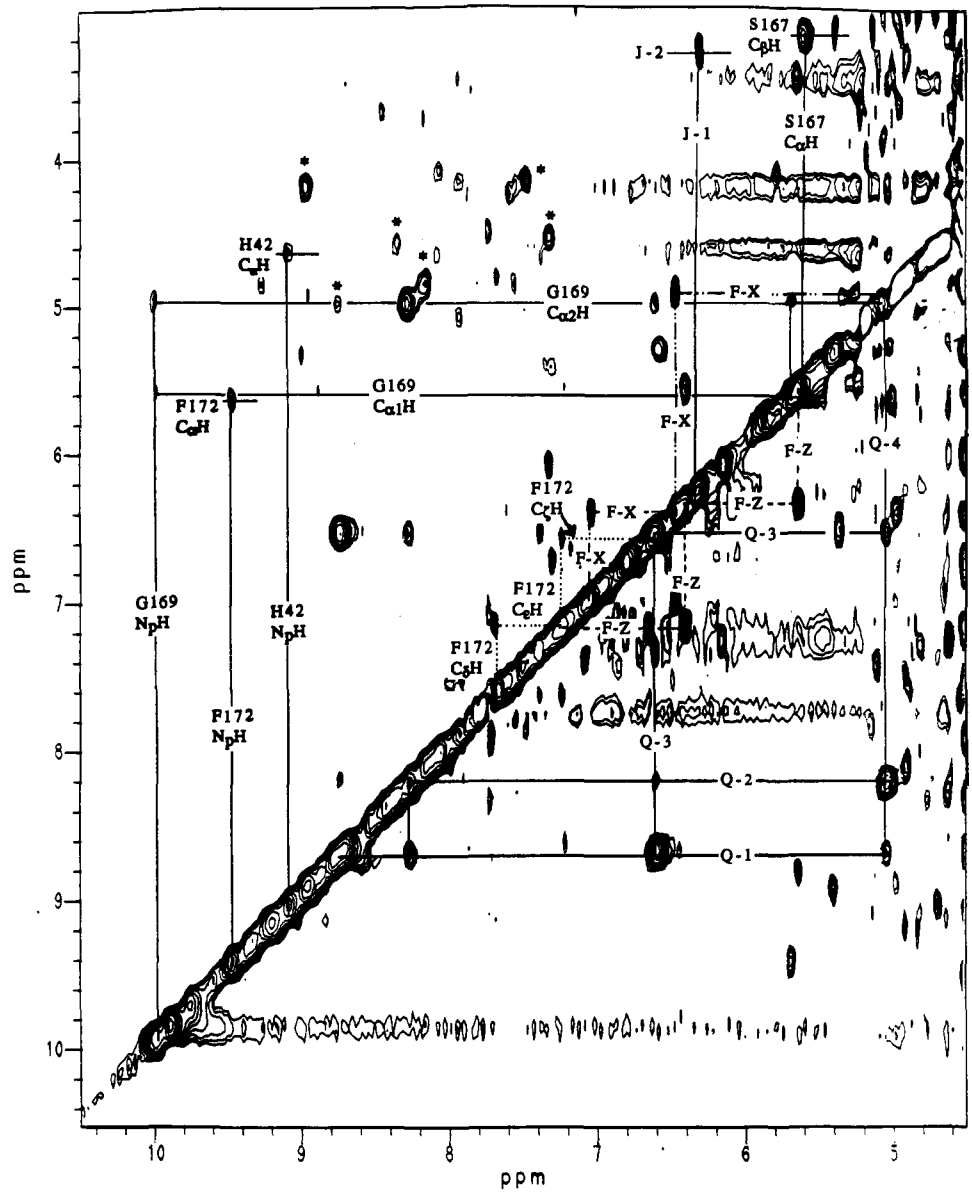

Figure 6. Portion of the 500 MHz ^{1}H CLEAN-TOCSY[27] spectrum of HRP–CN in ^2H_2O, pH 7.0, 55 °C, recorded with a 12 ms mixing time. Solid lines show the NpH–C_αH correlations, as well as the spin systems of residues J, Q, and Ser 167. Phe cross peaks for the aromatic rings are connected for Phe 172 (···), Phe-X (–···–), and Phe-Z (- - -). Asterisks indicate unassigned NpH–C_αH correlations. Assignments are given in text.

an Ile (Figure 7B). Further scalar connectivities to locate the remainder of the Ile spin system cannot be detected at this time in the crowded aliphatic spectral window. A third cross peak to the $C_\delta H_3$ is observed in the MCOSY spectrum (not shown; see supplementary material), where a strong NOESY peak is also detected (Figure 8A). It is clear that the third MCOSY peak is due to cross correlation with the likely $C_\gamma H_3$ of the same Ile, which is expected to be very near to $C_\delta H_3$.

One additional residue is located that exhibits both large hyperfine shifts and strong dipolar contact to His 170 C_βHs (Figure 5E). This residue, which we label Q, exhibits a four-spin system in TOCSY and NOESY spectra (resonances labeled Q-1-Q-4 in Figures 5 and 6). The relatively narrow line widths of the Q resonances (in steady-state NOEs; not shown) and suppressed intensity in the DEFT/WEFT traces in Figures 2C-E indicate a residue distant from the iron (>6.5Å). The relative intensities of cross peaks and variable temperature intercepts in the aliphatic region, rather than methyl or amide region (Table 1), suggest the presence of a $CHCH_2CH$ fragment.[40] The missing additional cross peak(s) are likely suppressed by long relaxation times or lost in the crowded aliphatic region.

Distal Side Residues. The 12 ms mixing time CLEAN-TOCSY[27] spectrum for the upfield window where the protons for Arg 38 resonate is shown in Figure 7B, with the relevant portion of the reference trace given in Figure 7A. The connecting lines show all of the necessary cross peaks for uniquely identifying an eight-spin system, although that for $C_{\gamma 1}H$–$C_{\gamma 2}H$ (where $C_{\gamma 2}H$ has one of the largest line widths and shortest[10a] T_1s (15 ms) in HRP–CN) can only be seen in the slice through $C_{\gamma 1}H$ (Figure 7C). The TOCSY map dictates that the low-field peak at 5.67 ppm, previously assigned as the Arg 38 C_αH based on NOESY data,[10a] *must actually be the peptide NH*, and that the C_αH is located with shift closer to $C_{\gamma 1}H$. This is confirmed in the NMR trace of the exchanged sample in Figure 2B, which clearly shows the loss of intensity for the 5.67 ppm peak. Nevertheless, CLEAN-TOCSY maps out the complete eight-spin system for Arg 38, the residue with some of the broadest resonances in HRP–CN, and again demonstrates the utility of this experiment for elucidating scalar correlations in a low-spin peroxidase. It is likely that the

(40) The presence of artifacts in the diamagnetic window in slow repetition rate NOESY spectra, and the partial suppression of the cross peaks for residue Q in WEFT- or DEFT-NOESY spectra, precluded definitive determination of which protons form a geminal pair.

Table 1. ^1H NMR Spectral Parameters for Heme Pocket Amino Acid Residues for HRP–CN at 45 °C, pH 7.0

	assignment	chemical shift[a] (ppm)	slope[b] (ppm·K × 10^3)	intercept[a,c] (ppm)
proximal residues				
Gly 169	N_pH	10.12	1.87	4.25
	$C_{\alpha 1}H$	5.73	1.67	0.50
	$C_{\alpha 2}H$	4.99	0.96	1.98
His 170	N_pH	12.16	3.02	2.67
	$C_\alpha H$	9.49	3.44	1.29
	$C_{\beta 1}H$	14.18	4.90	−1.21
	$C_{\beta 2}H$	21.44	8.85	−6.40
	$C_\epsilon H$	−27.4	−12.2	11.0
	$C_\delta H$	21.7	10.0	−9.8
Ser 167	$C_\alpha H$(?)[d]	5.73	1.46	1.15
	$C_\beta H$(?)[d]	3.26	0.52	1.62
Thr 171	N_pH	9.05	1.37	4.77
	$C_\alpha H$	5.04	0.42	3.73
Phe 172	N_pH	9.49	1.06	6.17
	$C_\alpha H$	5.65	0.36	4.55
	$C_\delta Hs$	7.61	0.41	6.35
	$C_\epsilon Hs$	7.16	−0.42	8.47
	$C_\zeta H$	6.53	−0.73	8.82
Residue-Q	Q-1	8.87	1.97	2.69
	Q-2	8.32	1.47	3.73
	Q-3	6.59	0.91	3.74
	Q-4	5.10	0.30	4.15
Ile 244	$C_\delta H_3$	−2.87	−1.57	2.05
	$C_\gamma H$	0.21	−0.25	1.00
	$C_\gamma H'$	1.17	−0.31	2.15
	$C_\gamma H_3$	1.35	−0.76	3.73
distal residues				
Arg 38	N_pH	5.67	−0.81	8.21
	$C_\alpha H$	0.59	−1.01	3.77
	$C_{\beta 1}H$	−4.91	−2.43	2.70
	$C_{\beta 2}H$	−0.59	−0.41	0.67
	$C_{\gamma 1}H$	0.61	1.42	−3.82
	$C_{\gamma 2}H$	−1.40	0.70	−3.63
	$C_{\delta 1}H$	−6.56	−2.02	−0.22
	$C_{\delta 2}H$	1.02	0.60	−0.90
Phe 41	$C_\beta H$	2.65	−0.31	3.63
	$C_\delta Hs$	7.62	0.71	5.39
	$C_\epsilon Hs$	6.34	0.86	3.64
His 42	N_pH	9.09	0.86	6.40
	$C_\alpha H$	4.76	0.83	2.14
	$C_\delta H$	10.03	2.12	3.37
	$C_\epsilon H$	12.70	2.29	5.49
	$N_\delta H$	16.08	1.77	10.51
	$N_\epsilon H$	29.78	11.04	−4.92
Residue-J	J-1	6.41	1.25	2.48
	J-2	3.27	0.73	0.98
peripheral residues				
Phe-W	ring-Hs	7.73	0.00	7.73
Phe-X	$C_\delta Hs$ or $C_\zeta H$	4.77	−1.35	9.02
	$C_\epsilon Hs$	6.37	−0.73	8.66
	$C_\zeta H$ or $C_\delta Hs$	6.97	−0.31	7.95
Phe-Z (Phe 152?)	$C_\delta Hs$ or $C_\zeta H$	7.15	−0.20	7.79
	$C_\epsilon Hs$	6.25	−0.60	8.16
	$C_\zeta H$ or $C_\delta Hs$	5.44	−0.85	8.15
Residue T (Ile T?)	$C_\gamma H_3$	−0.74	0.50	0.85
	$C_\beta H$	0.67	0.94	−2.28

[a] Referenced to DSS, in ^2H_2O except for His 42 ring labile protons, which are in ^1H_2O. [b] Slope, in ppm·K (×10^3), from the linear plot of chemical shift versus reciprocal absolute temperature (Curie plot). [c] Extrapolated intercept at infinite temperature in the Curie plot. [d] Tentative assignment are indicated by a question mark in parentheses.

homologous distal Arg 48 assignment in CcP–CN[13c] is similarly in error for the $C_\alpha H$ peak.

The available data reveal an extended orientation for Arg 38 with disposition relative to the heme that is remarkably like that

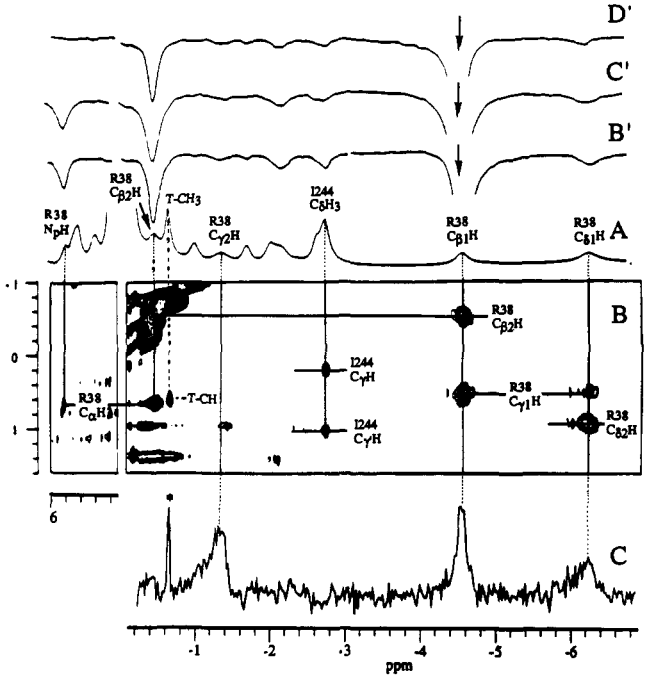

Figure 7. (A) Portion of the 500 MHz ^1H NMR spectrum of HRP–CN in ^2H_2O, 55 °C, pH 7.0. (B) CLEAN-TOCSY[27] spectrum collected with 12 ms mixing time and processed with 30°-shifted sine-bell-squared apodization in both dimensions showing scalar correlations for Arg 38, Ile 244, and Ile T. (C) f_2 slice through $C_{\gamma 1}H$ of Arg 38 from the TOCSY data of (B), but processed with 60°-shifted sine-bell-squared apodization in both dimensions. Traces B′–D′ are difference spectra from steady-state NOE experiments where the Arg 38 $C_{\beta 1}H$ was irradiated (indicated by arrow) for (B′) HRP–CN dissolved in ^2H_2O for ~ 1 month; (C′) HRP–CN in ^2H_2O stored for eight years at 5 °C, and (D′) HRP–CN reconstituted from apoprotein pretreated with ^2H_2O to exchange slowly exchanging peptide protons.[8d]

of the distal Arg in both CcP[3] and LiP.[6] The NOE and relaxation properties, moreover, result in stereospecific assignments.[37] The very strong NOESY cross peaks from Arg 38 $C_\beta Hs$ to Arg 38 N_pH (Figure 8A) are consistent with short distances (~2.5 Å) as in CcP (or LiP). The stronger NOE to 5-CH_3 and $6H_\beta s$ for the upfield Arg 38 $C_{\beta 1}H$ compared to the lower field $C_{\beta 2}H$ (Figures 8A,B) is also consistent, with $C_{\beta 1}H$ closer to the heme. The stronger NOESY peak to $C_\alpha H$ from $C_{\beta 1}H$ than $C_{\beta 2}H$ fits with ~2.6 vs 3.1 Å distances in CcP or LiP. The short T_1s for the high-field resolved $C_{\gamma 2}H$ (T_1 ~15 ms) and $C_{\delta 1}H$ (T_1 ~20 ms) are consistent with the proximity of these protons to the iron (R_{Fe} ≈ 4.2 ± 0.1, 4.5 ± 0.2 Å) in CcP and LiP. The intra-Arg and Arg–heme NOESY cross peaks, as well as the paramagnetic relaxation properties, are consistent with an extended Arg 38 configuration over pyrrole C that is remarkably similar to that observed in both CcP and LiP[3,6] (see Figure 1).

The distal His 42 ring was originally identified[8d] by observing steady-state NOEs from two hyperfine shifted and relaxed labile protons to two narrow, nonlabile protons (one resolved) in a pattern that dictated that the four protons arise from a protonated His side chain; moreover, the presence of a hydrogen bond between the $N_\epsilon H$ and the ligated cyanide could be demonstrated.[8d] These relevant NOESY cross peaks are readily detected in ^1H_2O (see supplementary material). The His 42 $C_\delta H$ exhibits a relatively strong NOESY cross peak[38] to a slowly exchanging labile proton at 9.09 ppm (Figure 5C and supplementary material), which, in turn, exhibits a TOCSY cross peak to 4.76 ppm (Figure 6) and hence identifies a $C_\alpha HN_pH$ fragment. The strong His 42 $C_\delta H$ NOE to this labile proton demands that this $C_\alpha HNH$ fragment arise from the same His 42; the predicted His 42 $C_\delta H$–N_pH distance is ~2.5 Å in the homologous residues in CcP[3] and LiP.[6] The His 42 $C_\beta Hs$ are expected to be much further from the iron (~9 Å) and are less strongly relaxed and hence likely do not

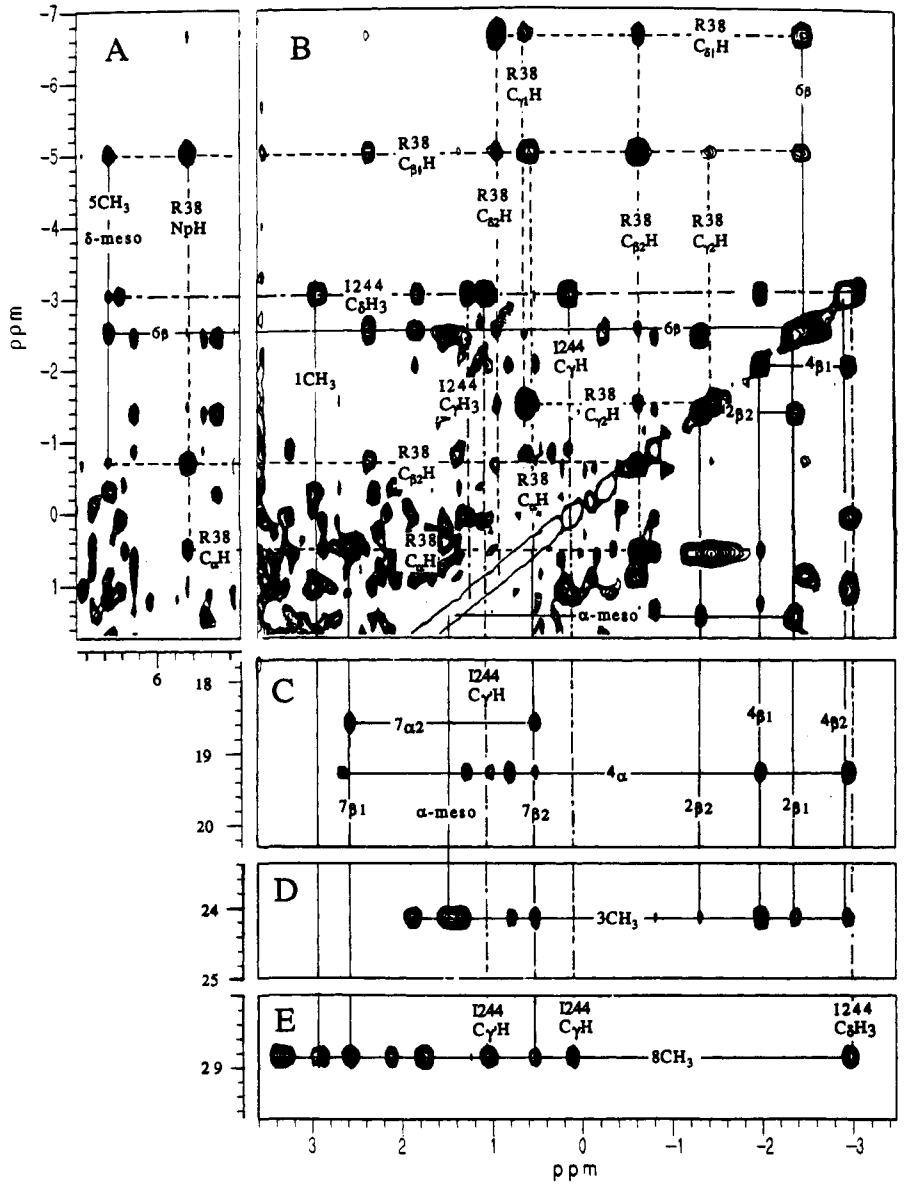

Figure 8. Portions of the 500 MHz ^{1}H NMR WEFT-NOESY spectrum of HRP–CN in ^2H_2O, 45 °C, pH 7.0, showing primarily correlations to upfield shifted protons. Data collected with a 20 ms mixing time and τ_{rd} = 160 ms. Cross peaks are labeled as in text and are connected by Arg 38 (- - -); Ile 244, (– · –) and heme (—). The only unassigned protons that exhibit cross peaks to resolved signals are protons with chemical shifts in the aliphatic window which exhibit minimal temperature dependence.

appear in the WEFT-NOESY map; they were not located. It is also noted that the His 42 $C_\delta H$ exhibits weak NOESY cross peaks to both $C_{\gamma 2}H$ and $C_{\gamma 1}H$ of Arg 38 (Figure 5A,C), exactly as predicted in *Cc*P and LiP (~3.2 Å).

His 42 $C_\delta H$ displays strong and weak NOESY cross peaks to two resonances in the aromatic spectral window at 7.62 and 6.34 ppm, respectively, which in turn exhibit a strong NOESY (but not MCOSY or TOCSY) cross peak between them (Figure 5C). These two signals, with relatively weak temperature dependent shifts (Table 1), but very strong paramagnetic relaxation, appear completely relaxed in the DEFT trace in Figure 2D, leading to estimated T_1s < 30 ms; the 7.62 ppm peak, moreover, exhibits closer to two-proton than one-proton intensity relative to the completely relaxed Arg 38 $C_{\delta 1}H$ peak (see Figure 2D,E). The relaxation properties dictate that the protons are <4.5 Å from the iron. The only protons that close to Fe in *Cc*P and LiP, and which have not already been assigned in HRP–CN, are from the side chain of the aromatic residue adjacent to the distal His, *i.e.*, Phe 41 (homologous to Trp 51 in *Cc*P[3] or Phe 46 in LiP[6]). The relaxation properties, relative intensity, relatively low-field intercepts in the Curie plot (Table 1), and NOESY pattern therefore strongly support the assignment of the 7.62, 6.34 peaks to the ring protons of a rapidly reorienting Phe 41. The NOESY cross peaks from the proposed aromatic ring to Arg 38 $C_\alpha H$, $C_{\gamma 2}H$ (Figures 5A,C), His 42 $C_\delta H$, N_pH (Figure 5C), and the heme 3-CH_3 (Figure 5F) place the ring near the distal Arg 38 and His 42 and over pyrrole B, as expected for Phe 41 (see Figure 1). The NOESY cross peaks from 7.62 ppm to both 3-CH_3 and Arg 38 $C_{\gamma 2}H$ are those expected for the averaged C_δHs (one is close to 3-CH_3, the other close to Arg 43 $C_{\gamma 2}H$ in LiP[6]), while the 6.34 ppm resonance can be attributed to the C_ϵHs based on its NOE to the C_δHs and a weak NOE to His 42 $C_\delta H$; the $C_\zeta H$ from Phe 41 was not located and is likely too close to the C_ϵHs peak to exhibit a cross peak. The strong NOE for the Phe 41 C_δHs to a moderately relaxed proton at 2.65 ppm locates the likely Phe 41 $C_\beta H$ (~2.6 Å in LiP[6]), which also exhibits the predicted strong NOEs to both His 42 $C_\delta H$ and N_pH (Figure 5C).

One additional distal residue (labeled J) is located with significant hyperfine shifts, as reflected in their temperature sensitivity (Table 1). Both His 42 $C_\epsilon H$ and $N_\delta H$ in ^1H_2O (supplementary material) and $C_\epsilon H$ in ^2H_2O (Figure 5D) exhibit

NOESY cross peaks to a peak at 6.41 ppm which exhibits a TOCSY (Figure 6) and NOESY (Figure 5C) cross peak to 3.27 ppm. The failure to detect additional TOCSY peaks precludes identifying the residue.

Peripheral Aromatic Residues. A resonance with temperature independent shift of 7.73 ppm with strong NOESY cross peaks to 8-CH_3 and 7$H_{\alpha 2}$ (supplementary material) was originally proposed[8c] to arise from Tyr 185 based on a computer model of HRP.[16a] This aromatic residue, which interacts with substrates, was later shown[16b,c] to be a Phe (we label it Phe-W) based on NOESY data in the presence of substrate and proposed to arise from Phe 142. ^{1}H NMR studies of the acidic A2 isozyme of HRP–CN reveal that a similar aromatic side chain does not make any contact with the pyrrole D substituents.[41] Since the sequences in the proposed active sites of the A2 and C isozymes,[5] their ^{1}H NMR spectra,[8,12] and most NOESY contacts (not shown[41]) are very similar, we conclude that Phe-W in isozyme C of HRP is substituted by an aliphatic residue in isozyme A2. Six Phe in isozyme C at positions 61, 68, 130, 143, 179, and 221 (HRP C numbering[5]) are replaced in isozyme A2. The conservation of Phe 142 argues against its assignment to Phe-W. Structural homology to isozyme E5 of HRP and C*c*P suggests Phe 61, 130 are too distant from the heme, leaving Phe 68, 143, 179, and 221 as viable candidates.

The 12 ms mixing time TOCSY map in Figure 6 labels the characteristic three resonances of two additional mobile phenyl groups with weakly temperature dependent shifts which extrapolate to the aromatic window[42] (Table 1) and are labeled Phe-X and Phe-Z. Phe-X exhibits weak upfield hyperfine shifts, and one of its resonances exhibits[43] strong NOESY contacts to 7$H_{\alpha 2}$ and 7$H_{\alpha 1}$ (supplementary material) at 45 °C. Phe-Z exhibits weak upfield hyperfine shifts and makes dipolar contact to the heme 3-CH_3 (Figure 5F) and 2-H_βs (Figure 5A), as reported previously.[17] The dipolar contacts to the heme indicate that the position of Phe-Z is similar to that occupied by Phe 158 in C*c*P[3], and hence has been attributed[17] to Phe 152 in HRP. The only additional data on Phe-Z is that it also makes dipolar contact with the upfield very weakly relaxed methyl peak at –0.74 ppm. This methyl resonance produces a single TOCSY cross peak (Figure 7B) to a proton at 0.67 ppm, with weakly temperature dependent shifts; the latter proton shows no other scalar connectivities to additional methyl resonances. The residue giving rise to the –0.74 and 0.67 ppm peaks is therefore more likely a Thr, Ile, or Ala than a Leu or Val. The relative upfield bias of the CH shift favors an Ile over a Thr or Ala, so we tentatively label the residue as Ile-T.

Heme Pocket Dynamics. It had been previously demonstrated that the axial His 170 peptide NH does not detectably exchange with ^2H_2O in the holoprotein, but that the exchange occurs readily in the apoprotein.[8d] The present results show that this dynamic stability is extended to a significant portion of the proximal helix. More surprisingly, the assignment of Arg 38 and His 42 peptide NHs in this work establishes that the extraordinary dynamic stability previously noted for the proximal environment of the heme pocket in the holoprotein extends to the distal side as well. Figure 7B′ and 7C′ display steady-state NOEs to the Arg 38 NpH upon saturating $C_{\beta 1}$H for two samples, one that had been in ^2H_2O for several weeks at 5 °C, pH 7.0 (Figure 7B′) and another sample in ^2H_2O stored for 8 years at 5 °C, pH 7.0. It is noted that the intensity loss of the peptide NH over 8 years is negligible (judged ≤5%), indicating that the half-life for exchange under these conditions is >80 years! Since solvent has ready access at least to the distal pocket, as witnessed by the relatively rapid exchange with water of the His 42 side chain NHs,[8d] the extremely slow exchange rates for the nearby peptide NHs in the pocket must reflect the inherent dynamic stability of the protein secondary structure. The extraordinary stability of its secondary structure, however, is contrasted with the narrow lines for several very mobile heme pocket Phe.[16b,c] The latter property is likely a requirement for the effective binding for a variety of aromatic substrates.[1]

The detection of numerous slowly exchanging peptide NH protons in the active site of HRP–CN has an experimental advantage for pursuing further 2D NMR molecular structure determination[20] in heme peroxidases in general. In ^1H_2O, homonuclear ^{1}H sequence specific assignments of residues using the backbone dipolar connectivities are severely complicated by spectral overlap in the crowded peptide NH region of a 308 residue protein. However, the observed localization of the relatively few slowly exchanging protons present in ^2H_2O to the heme pocket should allow a more extensive investigation of the active site by sequence specific assignments in ^2H_2O that could allow additional assignments for nearby residues which exhibit negligible hyperfine shifts or paramagnetic relaxation. Such studies are in progress.

Heme Pocket Structure. The distal His and Arg are completely conserved in the plant, fungal, and bacterial peroxidases.[1,5] Moreover, the stereochemistry of these two residues relative to each other and to the heme in the crystal structures of C*c*P[3] and LiP[6] are essentially identical. Arg 38 in HRP exhibits heme contacts to 5-CH_3 and 6H_βs (as shown in Figures 8A,B) which indicate a completely conserved disposition relative to the heme when compared to both C*c*P[3] and LiP[6]. The earlier relaxation data[8d] on the labile protons on the imidazolium ring of His 42, together with the presently observed dipolar contacts from His 42 C_δH to Arg 38 $C_{\gamma 1}$H, $C_{\gamma 2}$H (Figure 5A,C), as well as to its own peptide NH (Figure 5C), again support a geometry for the distal His remarkably similar to that in C*c*P[3] or LiP[6]. The aromatic residue adjacent to the distal His is Trp 51 in C*c*P[3] and Phe 46 in LiP[6] and, hence, does not allow a direct comparison of Phe 41 of HRP with both structurally characterized enzymes. When the phenyl ring is substituted (using the Biosym Insight II program) directly for the Trp 51 side chain in C*c*P, with conserved C_α–C_β bond angle, the phenyl side chain position relative to the heme and the distal His and Arg differs from that in LiP, as shown in Figure 1. The alternate orientations predict distances to the iron[44] which differ insufficiently to distinguish between the two possible orientations of Phe 41 in HRP based on relaxation data; both are qualitatively consistent with the estimated T_1s. However, inspection of the Phe 41 ring proton distances to both His 42 and Arg 38 in the two alternate orientations reveals that two such distances[45] vary significantly between the two geometries. The distance between His 42 C_δH and Phe 41 C_ϵH is 2.1 Å in the C*c*P and ~5 Å in the LiP orientation of the phenyl group, while that between Arg 38 C_αH and Phe 41 C_δH is 2.6 Å in C*c*P

(41) Chen, Z.; de Ropp, J. S.; La Mar, G. N. Unpublished data.

(42) One additional Phe side chain, designated Phe-Y, with essentially temperature-independent chemical shifts of 7.92, 7.05, and 6.30 ppm at 45 °C, yields the expected two TOCSY peaks with an 8 ms but not with a 12 ms mixing time TOCSY spectrum (not shown), indicating that the line widths are greater (shorter T_2) than for Phe-W, -X and -Z. The expected NOESY cross peaks are clearly observed in a normal NOESY spectrum (not shown), but are sharply suppressed or undetectable in the WEFT- or DEFT-NOESY spectra, dictating that the protons are very inefficiently relaxed by the iron. The properties of Phe-Y in the TOCSY and NOESY experiments indicate that the side chain is relatively immobile when compared to that for Phe-W, -X, and -Z and remote from the heme pocket. Hence, Phe-Y is not considered further.

(43) The NOESY cross peak between Phe-X and the heme 7$_{\alpha 2}$H could not be confirmed at temperatures other than 45 °C, in spite of significant temperature dependence to both shifts, because of overlap of the cross peaks with many others in the same region. Hence, its location in the heme pocket must be considered tentative, although strongly supported by the obvious hyperfine shifts.

(44) The closest distal Phe ring proton to iron is 4.6 ± 0.1 Å for C_δH in C*c*P (substituted for Trp 51) and LiP, which is consistent with the estimated T_1 ≤ 30 ms. The closest approach to the iron for C_ϵH (when rotating the α–β bond) varies from 3.2 Å in C*c*P (with Phe 51) to 4.5 Å in LiP, but the C_ϵH T_1 could not be estimated.

(45) The other relevant detected NOESY cross peaks (cross peak intensity; separation in C*c*P, LiP) are His 42 C_δH-Phe 41 C_δH (strong; 2.0 ± 0.1 Å), Phe 41 C_δH-3-CH_3 (weak; 3.4 ± 0.1 Å), Phe 41 C_δH-Phe 41 C_βH (strong; 2.3 Å); Phe 41 C_δH-His 42 NpH (weak; 3.6 ± 0.2 Å).

and 4.9 Å in LiP. Since the observed NOESY cross peaks for these two pairs of protons are weak (Figure 5C), the NOESY data favor an orientation for Phe 41 in HRP relative to the heme distal Arg and His that is between those predicted for CcP and observed in LiP[6], but much closer to the latter. The distal residue *J*, with proximity to the distal His 42 $N_\delta H$ and $C_\epsilon H$, occupies a region of space where there is little sequence homology among the three proteins.[1,5] Since only a portion of the spin system could be detected, it is premature to speculate on its side chain origin.

The orientation of the axial His 170 relative to the heme in HRP–CN has already been shown to resemble closely that of CcP–CN[3], as evidenced by the heme methyl contact shift pattern (large 3-CH_3, 8-CH_3 shifts[8a,10a,13]) that is known to be related to the orbital ground state,[46] which in turn is largely determined by an axial His imidazole orientation[47] that must be close to parallel to the pyrrole A–C vector (see Figure 1). The present observation of a NOESY cross peak between the Gly 169 NH and the 4-vinyl $H_{\beta 1}$ (Figure 5A) is consistent with that expected for the homologous Ala 174 in CcP (Figure 1). The remainder of the identified proximal helix residues do not, and are not expected to, exhibit NOESY cross peaks to the heme. The proximal residue whose methyl is in contact with the pyrrole A, D junction, which has been demonstrated to be near the substrate binding site,[2,8c] is clearly shown to be an Ile. This Ile occupies a position in the pocket of HRP that is held by Ile 235 in LiP[6] and Leu 232 in CcP[3] and, hence, is assigned to the homologous Ile 244, as proposed earlier.[17]

The proximal residue-Q, which exhibits strong dipolar contact with the His 170 $C_\beta Hs$, occupies a position homologous to Phe 202 in CcP[3] and Phe 204 in LiP[6] (Figure 1), both of which reside on helix G. The proposed homologous sequence in HRP does not contain a Phe,[1,5] and this portion of the molecule is still poorly defined in the E5 HRP X-ray structure.[7] The relatively narrow peak line widths and Curie plot intercepts (Table 1), as well as the TOCSY (Figure 6) and NOESY (Figure 5C) cross peak patterns, indicate a residue that contains a $CHCH_2CH$ fragment,[40] which is inconsistent with a Phe, but suggests Glu, Gln, Leu, Arg, Lys, Met, or Pro. Considerably more 2D NMR data are needed to unambiguously identify residue Q.

(46) Shulman, R. G.; Glarum, S. H.; Karplus, M. *J. Mol. Biol.* **1971**, *57*, 93–115.
(47) Rajarathnam, K.; La Mar, G. N.; Chiu, M. L.; Sligar, S. G. *J. Am. Chem. Soc.* **1992**, *114*, 9048–9058.

Conclusions

2D NMR methods appropriately tailored to enhance cross peaks from protons which are rapidly relaxed and/or exhibit strongly temperature dependent shifts, together with backbone sequential assignments for slowly exchanging peptide NHs, are shown to lead to the assignment of the majority of the active site residues of HRP–CN. The approaches described herein lead to the identification of all hyperfine-shifted resonances which exhibit NOESY cross peaks to the heme and axial His (Figures 5, 7, and 8). It is concluded that TOCSY, but not conventional COSY, experiments are necessary and sufficient to uniquely map scalar connectivities in a variety of low-spin heme peroxidases in size to ~44 kDa.[8,10,12,13,15] However, neither TOCSY nor COSY are likely useful for the much larger mammalian peroxidases.[14] The orientations in the active site of the conserved catalytically important distal His and Arg in HRP are shown to be essentially identical to those observed in both CcP[3] and LiP.[6] In a separate report, we show that the structural elements in HRP conserved with respect to CcP and LiP allow the development of a semiquantitative interpretative basis for all hyperfine shifts in low-spin heme peroxidases that reflect on distal steric and/or hydrogen bonding effects on the coordinated ligand.[23]

Acknowledgment. The authors are indebted to Drs. M. Sette and S. C. Busse for the suggestion of DEFT and WEFT 2D experiments and to Dr. J. Qin for valuable discussions. This research was supported by a grant from the National Institutes of Health, GM 26226. The GE Ω-500 spectrometer was purchased in part with funds from the National Institutes of Health, RR-04795, and the National Science Foundation, BBS-88-04739.

Supplementary Material Available: Figures showing the high-field and low-field portions of the ^1H MCOSY, ^1H CLEAN-TOCSY, low-field portions of the ^1H NMR NOESY, and portions of the WEFT-NOESY spectra of HRP-CN, P-COSY f_1 slices for HRP-CN, and NOESY f_2 slices through the Phe 41 $C_\beta H$ diagonal (7 pages). This material is contained in many libraries on microfiche, immediately follows this article in the microfilm version of the journal, and can be ordered from the ACS; see any current masthead page for ordering information.